Journal of Catalysis **212,** 39–45 (2002)
doi:10.1006/jcat.2002.3756

Oxidation of Cyclohexane, Cyclohexanone, and Cyclohexanol to Adipic Acid by a Non-HNO_3 Route over Co/Mn Cluster Complexes

S. A. Chavan, D. Srinivas, and P. Ratnasamy[1]

National Chemical Laboratory, Pune 411 008, India

Received February 4, 2002; revised July 18, 2002; accepted July 25, 2002

μ_3-Oxo-bridged Co/Mn cluster complexes, $CoMn_2(O)$, exhibit high catalytic activity and selectivity for the aerial oxidation, in the homogeneous liquid phase, of cyclohexane, cyclohexanol, and cyclohexanone to adipic acid by a non-HNO_3 route. The cluster complexes are superior to the individual Co and Mn acetates. The yields of adipic acid are comparable to those in the current processes using HNO_3. Electron paramagnetic resonance and electronic spectra indicate that the cluster complex is probably decomposed during the reaction process. Attempts to use these cluster complexes encapsulated in zeolite–Y as solid catalysts for the oxidation reactions were unsuccessful due to significant leaching out of the complexes during the reaction.

Key Words: **aerial oxidation; oxidation of cyclohexane, cyclohexanol, and cyclohexanone; oxidations over μ_3-oxo-bridged Co/Mn cluster complexes; adipic acid via a non-HNO_3 route.**

INTRODUCTION

Adipic acid (AA), a valuable raw material used in the production of nylon-6,6, fibers, plasticizers, and food additives, is manufactured by the oxidation of cyclohexanone, obtained either by hydrogenation of phenol or, more commonly, by the oxidation of cyclohexane (1–3). In the first stage, cyclohexane is oxidized with oxygen (423–473 K; 115–175 psig), using a soluble cobalt catalyst (usually cobalt naphthenate, cobalt octonate, or cobalt acetate) to a mixture of cyclohexanol–cyclohexanone (referred to as KA oil; conversion <10%; selectivity ≈70–90%). In the second stage, this mixture is further oxidized, at 343–364 K, to AA (yield of AA = 70–95%) by 40–60% HNO_3 in the presence of copper and vanadium catalysts (2). During the second stage, significant amounts of environmentally harmful NO_x effluents (NO, NO_2, and N_2O) are produced (4, 5). While NO and NO_2 are recycled to the HNO_3 plant, N_2O is usually vented and constitutes a major source of this highly polluting species. According to the global warming treaty signed in Kyoto all the AA manufacturers had to install N_2O removal systems by the end of 2000, adding cost to the existing technology. Asahi Chemical Industry, BASF, Bayer, and DuPont employ catalytic or thermal processes to destroy the N_2O (6). Solutia and Rhodia subsidiary Alsachimie (Chalampe, France) recycle the N_2O back into their production processes (phenol and HNO_3, respectively). An alternative non-HNO_3 route to AA using cleaner oxidants such as O_2 or H_2O_2 is highly desirable.

Although many variations of the initial cyclohexane oxidation (to KA oil) step have been developed, technology for the second stage (conversion of KA oil to AA) is fundamentally the same as originally developed by Du Pont in the early 1940s (1). A number of alternative processes for producing AA have been investigated but none of them has been commercialized so far (7–9). Tanaka (7, 8) has reported a single-step, liquid-phase, aerial oxidation of cyclohexane to AA (yields of AA = 70–75% at cyclohexane conversions of 50–75% and 343–373 K). BASF has developed a process based on hydrocarboxylation or carboalkoxylation of butadiene (9). Jacobs and coworkers (10–12), Balkus and coworkers (13, 14), Herron *et al.* (15) and Raja and Ratnasamy (16, 17) studied this oxidation with *tert*-butylhydroperoxide or iodosylbenzene over metal phthalocyanine complexes encapsulated in zeolite–Y. Sato *et al.* (18) oxidized cyclohexene with 30% H_2O_2 over $Na_2WO_4 \cdot 2H_2O$. Recently, Thomas and coworkers (19–21) and Luna *et al.* (22) oxidized cyclohexane and *n*-hexane with air to AA over metal-containing aluminium phosphate molecular sieves. However, none of these studies using solid catalysts has the potential to replace the current commercial process due to their low yields of AA and/or use of expensive oxidants such as H_2O_2, *tert*-butylydroperoxide, and iodosylbenzene.

In our studies on the oxidation of *para*-xylene to terephthalic acid we had reported (23) that μ_3-oxo-bridged cluster complexes (Fig. 1) are formed from Co and Mn acetates in acetic acid (HOAc) medium during the oxidation process. These complexes (especially the heteronuclear $CoMn_2(O)$), in both neat state and when encapsulated in zeolite–Y, exhibited higher activity and selectivity in the *para*-xylene oxidation than the individual metal acetates (24, 25). We now report the aerial oxidation of cyclohexanone, cyclohexanol, and cyclohexane to AA using these

---

[1] To whom correspondence should be addressed. Fax: +91-20-5893355. E-mail: prs@ems.ncl.res.in.

0021-9517/02 $35.00

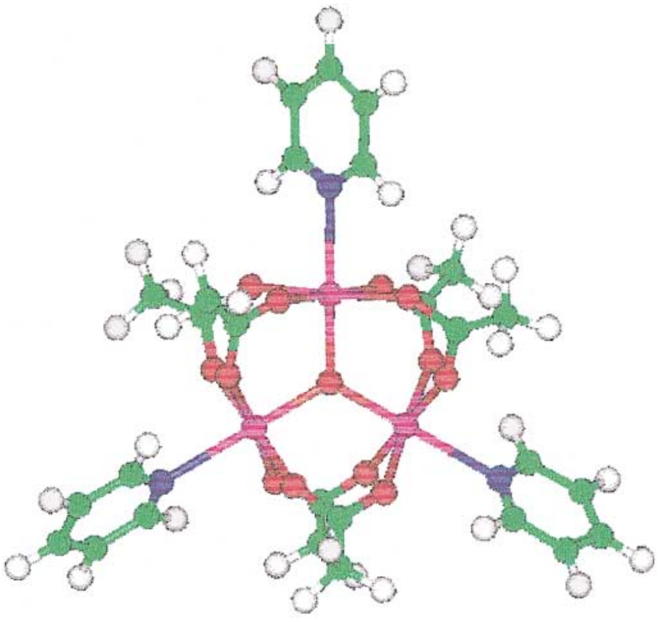

FIG. 1. Structure of μ_3-oxo-bridged Co/Mn cluster complex.

μ_3-oxo-bridged cluster complexes, $CoMn_2(\mu_3\text{-}O)(OAc)_6(py)_3$, $Mn_3(\mu_3\text{-}O)(OAc)_6(py)_3$, and $Co_3(\mu_3\text{-}O)(OAc)_6(py)_3$ (hereafter referred to as $CoMn_2(O)$, $Mn_3(O)$, and $Co_3(O)$, respectively; py = pyridine). To our knowledge this is the first non-HNO_3, aerial oxidation route for the preparation of AA from cyclohexanone wherein the yields of AA are comparable to those obtained in the current, commercial practice.

EXPERIMENTAL

The "neat" and zeolite–Y-encapsulated μ_3-oxo-bridged cluster complexes ($CoMn_2(O)$, $Mn_3(O)$, and $Co_3(O)$) were prepared and characterized as reported earlier (25).

Procedures

FT-IR spectra of the complexes were recorded on a Shimadzu FT-COM 1 spectrophotometer as Nujol mulls. UV–visible spectra were measured using a UV-101PC spectrophotometer. EPR spectra were recorded using an X-band Bruker EMX spectrometer (23).

Catalytic Activity Studies

The oxidation reactions were conducted in a titanium-lined Parr 4843 reactor. In a typical reaction 4.21 ml of cyclohexanone, 4.3 ml of cyclohexane, or a mixture of cyclohexanol and cyclohexanone was taken in 38 ml of glacial HOAc and 1.9 ml of distilled water; 0.114 ml of methylethylketone (MEK; oxidation initiator) and a known amount of the catalyst were then added. The reactor was pressurized with air to 700 psig and heated to 373 K. After 4 h, the reactor was cooled to 298 K and the conversion of reactant(s) and liquid products formed were determined by gas chromatographic analysis. In the case of cyclohexane oxidation the catalytic runs were conducted for 8 h. The main reaction products were adipic, valeric, glutaric, and succinic acids. These acids were analyzed by GC and identified by GC–MS after esterification with BF_3 (23). Mass balances were verified. Addition of water controls the oxidation of HOAc to CO_2 and CO in the Co/Mn catalyzed reactions (26). Blank, controlled experiments were conducted with no catalyst. The reactions did not proceed in the absence of any catalyst, indicating that they are catalytic in nature.

Caution! The oxidation reactions are potentially explosive and necessary care and safety precautions should be taken (1, 3).

RESULTS AND DISCUSSION

Characterization of μ_3-Oxo-Bridged Co/Mn Cluster Complexes (24, 25)

The cluster complexes showed IR peaks at 1605 and 1404 cm^{-1} for $Mn_3(O)$, 1609 and 1402 cm^{-1} for $Co_3(O)$, and 1616 and 1604 cm^{-1} for $CoMn_2(O)$ due to the asymmetric and symmetric stretching vibrational modes of the COO^- group of acetate ligands (Fig. 2). The separation between $\nu_{as}(COO^-)$ and $\nu_s(COO^-)$ indicates bidentate coordination of acetate molecules, in *syn–syn* mode, to the metal ions. The characteristic peak of the μ_3-oxo-bridge (sensitive to the coordinated metal ion) appeared at 665, 692, and 685 cm^{-1} for $Mn_3(O)$, $Co_3(O)$, and $CoMn_2(O)$, respectively (Fig. 2).

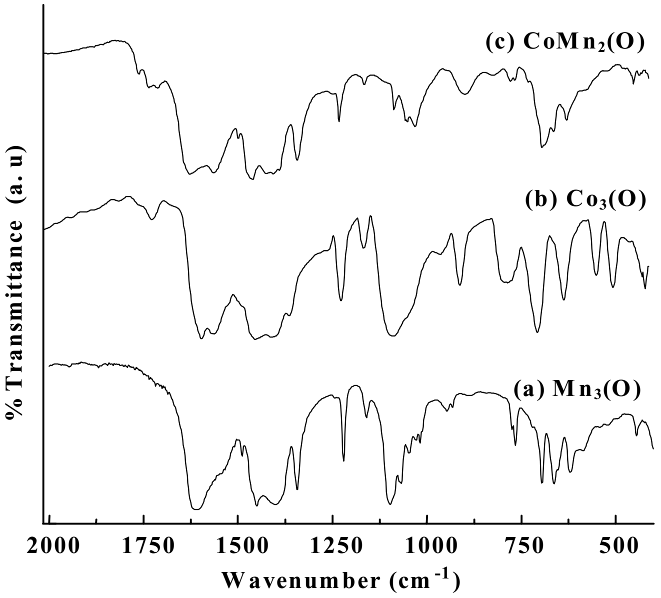

FIG. 2. FT-IR spectra (Nujol mull) of μ_3-oxo-bridged cluster complexes.

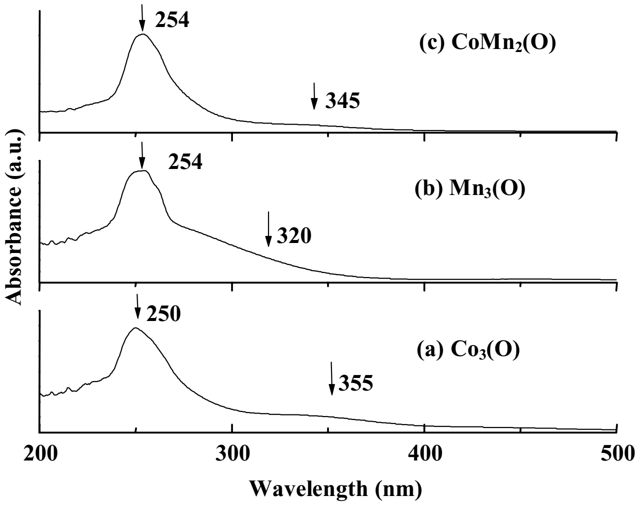

FIG. 3. UV–visible spectra of μ_3-oxo-bridged cluster complexes in HOAc.

TABLE 1

Selective Oxidation of Cyclohexanone over μ_3-Oxo-Bridged Co/Mn Cluster Complexes[a]

Run no.	Catalyst	Temp. (K)	Conv. (wt%)	TOF[b]	Product distribution (wt%)			
					SA	GA	VA	AA
1	Co$_3$(O)	363	11.9	136	10.6	15.1	0	74.3
2	Mn$_3$(O)	363	93.7	1104	3.0	13.9	0	83.1
3	CoMn$_2$(O)	353	82.8	941	5.2	18.7	1.1	75.0
4	CoMn$_2$(O)	363	92.2	1048	6.9	14.7	0	78.4
4a	CoMn$_2$(O)	363	90.1	1024	2.3	14.4	3.3	80.0
5	CoMn$_2$(O)	373	97.6	1104	1.9	11.5	0	86.6
6	CoMn$_2$(O)	423	99.9	1130	6.6	21.5	4.7	67.2

[a] Reaction conditions: catalyst weight = 7.5 mg (8.6–8.9 μmol); cyclohexanone = 4.21 ml (40.5 mmol); oxidant = air (550 psig when hot); oxidation initiator = MEK (0.114 ml); medium = HOAc (38 ml) + water (1.9 ml); reaction time = 4 h. Run 4a was without MEK.

[b] Turnover frequency (TOF) = number of moles of substrate converted per mole of the catalyst per hour.

The acetic acid solutions of the cluster complexes showed a partially resolved UV band, characteristic of a μ_3-oxo bridge, at around 320 nm for Mn$_3$(O) and 355 and 345 nm for Co$_3$(O) and CoMn$_2$(O), respectively (Fig. 3). The position of this band, attributed to oxygen-to-metal charge transfer, is sensitive to the coordinated metal ion.

Detailed EPR spectroscopic studies of the cluster complexes have already been reported by us earlier (25). Spectral variations in the range 77–298 K were consistent with intermolecular antiferromagnetic interactions (25). Polycrystals of Mn$_3$(O) complex showed a broad, isotropic signal at $g = 2.01$ with a peak-to-peak linewidth of 500 G. Co$_3$(O) cluster complexes also showed an isotropic signal ($g_{\mathrm{iso}} = 2.259$), but with a linewidth of 1075 G. CoMn$_2$(O) clusters were EPR silent.

Oxidation of Cyclohexanone

Effect of cluster composition and reaction temperature. Adipic acid (AA) was the major product while succinic (SA), glutaric (GA), and valeric acids (VA) were the minor products in the oxidation of cyclohexanone. The composition of the cluster complex has a marked effect on the reactivity (conversion and TOF) and product selectivity. Table 1 lists the catalytic activity data of the cluster complexes. Though Mn$_3$(O) and CoMn$_2$(O) clusters exhibit similar activity, the yield of AA was more with the former (Table 1, Runs 2 and 4). Among the three clusters, Co$_3$(O) exhibited least activity and AA selectivity (Table 1, compare runs 1, 2, and 4). On increasing the temperature from 353 to 423 K, while the conversion and TOF of cyclohexanone increased, the yield of AA passed through a maximum around 373 K (Table 1, Runs 3–6).

Effect of pressure and reaction time. The conversion of cyclohexanone and AA yield increased with pressure (from 200 to 900 psig) and reaction time (Table 2). Under our reaction conditions, complete conversion of cyclohexanone was achieved at 6 h (Table 2, Run 12). Product selectivity, however, was less sensitive to changes in pressure and reaction time.

Oxidation of a Mixture of Cyclohexanone and Cyclohexanol

The oxo-bridged clusters are highly efficient in the oxidation of cyclohexanone–cyclohexanol (-one/-ol) mixtures. While the ketone (-one) is oxidized directly to the acid products, the alcohol (-ol) is oxidized initially to -one and then, subsequently, to the acid products (1–3). The catalytic

TABLE 2

Effects of Pressure and Reaction Time on Product Distribution in the Oxidation of Cyclohexanone: Catalyst, CoMn$_2$(O); temperature, 363 K[a]

Run no.	Pressure (psig)	Reaction time (h)	Conv. (wt%)	TOF	Product distribution (wt%)			
					SA	GA	VA	AA
1	200	0.75	51.6	3112	0	14.7	5.8	79.5
2	350	0.75	71.0	4282	1.0	13.1	5.7	80.3
3	550	0.75	89.8	5415	2.9	15.7	1.7	79.7
4	700	0.75	94.9	5723	3.2	14.9	3.0	79.0
5	900	0.75	98.2	5922	3.0	13.2	3.8	80.0
6	550	0.25	69.5	12573	3.0	14.9	1.9	80.2
7	550	0.50	84.7	7662	2.7	13.0	2.1	82.1
8	550	1.0	88.0	3980	3.3	15.1	2.1	79.5
9	550	1.5	89.1	2687	2.1	13.4	2.1	82.4
10	550	2	90.6	2049	3.0	15.3	3.3	78.4
11	550	3	90.0	1357	2.3	13.8	2.2	81.7
12	550	6	99.9	755	3.6	17.1	3.0	76.3

[a] Other reaction conditions are the same as in Table 1.

TABLE 3

Selective Oxidation of a Mixture of Cyclohexanol (-ol) and Cyclohexanone (-one) over μ_3-Oxo-Bridged Co/Mn Cluster Complexes at 363 K[a]

Run no.	Catalyst	Substrate (-ol : -one)	Overall conv. (wt%)	Individual conv. (wt%)		Product distribution (wt%)			
				-ol	-one	SA	GA	VA	AA
1	CoMn$_2$(O)	0 : 100	92.2	—	92.2	6.9	14.7	0	78.4
2	CoMn$_2$(O)	10 : 90	85.9	100	84.5	3.3	17.5	1.4	77.9
3	CoMn$_2$(O)	20 : 80	84.5	100	80.9	3.4	15.2	1.7	79.7
4	CoMn$_2$(O)	50 : 50	79.1	91.3	65.5	3.3	12.5	1.7	82.5
5	Mn$_3$(O)	0 : 100	93.7	—	93.7	3.0	13.9	0	83.1
6	Mn$_3$(O)	10 : 90	87.1	100	86.1	2.9	16.7	0.8	79.6
7	Mn$_3$(O)	20 : 80	80.5	96.1	75.6	2.2	13.1	0.6	84.1
8	Mn$_3$(O)	50 : 50	84.7	94.7	74.1	2.3	13.3	0.8	83.7

[a] Run time = 4 h. Other reaction conditions are the same as in Table 1.

activity data are presented in Table 3. The conversion of -ol increased (from 91 to 100 wt% over CoMn$_2$(O) and from 94.7 to 100 over Mn$_3$(O)) with increasing concentration of -one in the reaction mixture (Table 3). In the absence of -one the conversion of -ol was very low (45 wt%). In contrast, the individual conversion of -one decreased (from 84.5 to 65.5 wt% over CoMn$_2$(O) and from 86.1 to 74.1 wt% over Mn$_3$(O)) with increasing concentrations of -ol in the reaction mixture (Table 3). In the absence of -ol the conversion of -one was higher (92.2 wt% over CoMn$_2$(O) and 93.7 wt% over Mn$_3$(O)). The overall conversion of the reaction mixture (-one + -ol) decreased from 92 to 79 wt% over CoMn$_2$(O) and from 93.7 to 84.8 wt% over Mn$_3$(O) with increasing -ol concentration. AA selectivities, however, are not significantly changed ($80 \pm 5\%$) (Table 3). It appears that -ol is a poison in cyclohexanone oxidation.

Oxidation of Cyclohexane

The catalytic activity of the cluster complexes in cyclohexane oxidation decreased in the order Co$_3$(O) > CoMn$_2$(O) > Mn$_3$(O) (Table 4). Succinic and glutaric acids were the major products. It may recalled that adipic acid is the major product in the oxidation of cyclohexanone–cyclohexanol (Tables 1–3).

TABLE 4

Aerial Oxidation of Cyclohexane over μ_3-Oxo-Bridged Co/Mn Cluster Complexes[a]

Run no.	Catalyst	Conv. (wt%)	TOF	Product distribution (wt%)					
				-ol	-one	SA	GA	VA	AA
1	Co$_3$(O)	85.6	489	5.0	1.5	16.2	55.0	0.4	22
2	Mn$_3$(O)	41.8	248	—	1.0	59.6	1.1	—	38.3
3	CoMn$_2$(O)	51.6	293	3.7	1.3	31.6	27.2	—	36.2

[a] Cyclohexane = 4.4 ml (40.7 mmol); reaction time = 8 h. Other reaction conditions are the same as in Table 1.

Oxidations over Mn$_3$(O), Co$_3$(O), and CoMn$_2$(O) Complexes Encapsulated in Zeolite–Y

The encapsulated cluster complexes were prepared as reported earlier (18). The encapsulated complexes exhibited activity (in cyclohexanone oxidation with conversion = 3.7, 97.1, and 98.4 wt% and AA selectivity = 91, 82.5, and 79.3 wt% for Co$_3$(O)–Y, Mn$_3$(O)–Y and CoMn$_2$(O)–Y, respectively) similar to that of the neat clusters. However, significant leaching out of the metal ions during the reaction was observed. This was in contrast to the situation in the oxidation of *para*-xylene at 473 K and 700 psig wherein such leaching was negligible (25). The reasons for these differences are under investigation.

In Situ Spectroscopic Studies

In situ electronic and EPR spectroscopic studies had enabled us, earlier, to identify the oxo-bridged clusters as the active species in *para*-xylene oxidation (23). Similar studies for cyclohexanone oxidation were performed on the following solutions:

1. Mn(OAc)$_2$ in HOAc + pyridine + water (298 K; 363 K for 45 min; 700 psig air, 363 K, 45 min).
2. Solution 1 + MEK (700 psig air, 363 K, 45 min).
3. Solution 2 + cyclohexanone (700 psig air, 363 K, 45 min).
4. A mixture of Co(OAc)$_2$ and Mn(OAc)$_2$ (3 : 1 mmol ratio) in HOAc + pyridine + water (298 K; 363 K for 45 min; 700 psig air, 363 K, 45 min).
5. Solution 4 + MEK (700 psig, 363 K, 45 min).
6. Solution 5 + cyclohexanone (700 psig, 363 K, 45 min).

Electronic Spectroscopy

Solution 1, containing Mn(OAc)$_2$, did not exhibit any absorption in the visible region. However, on heating at 363 K for 45 min and pressurizing with air (700 psig) a narrow band at 490 nm, a broad band at 445 nm, and a shoulder around

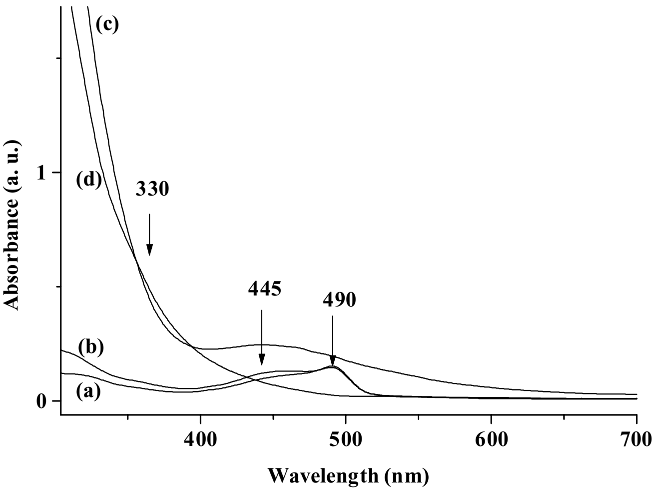

FIG. 4. Electronic spectra of manganese complexes: (a) $Mn(OAc)_2$ in HOAc + pyridine + H_2O at 363 K, 45 min; (b) solution in (a) at 700 psig air, 363 K, 45 min; (c) $Mn(OAc)_2$ in HOAc + pyridine + H_2O + MEK at 700 psig air, 363 K, 45 min; (d) $Mn(OAc)_2$ in HOAc + pyridine + H_2O + MEK + cyclohexanone at 700 psig air, 363 K, 45 min.

330 nm (Fig. 4, curves a and b) were observed. The former (490 nm) corresponds to *d–d* transition of a monomeric Mn(III) species. The latter two bands are attributed to *d–d* transition and oxygen ⇒ Mn(III) charge transfer transition of μ_3-oxo-bridged Mn cluster complex ($Mn_3(O)$); the assignment of the 330-nm band was also confirmed from $Mn_3(O)$ cluster complexes prepared independently (*vide supra*)). As anticipated, the intensities of $Mn_3(O)$ bands increased with the concentration of O_2 (higher pressure of air). When the experiment was conducted with MEK, the color of the solution changed from pale yellow to deep brown. Solution 2 showed intense bands at 445 and 330 nm due to $Mn_3(O)$ cluster complex (Fig. 4, curve c; dilution factor = 20). MEK promoted the oxidation of Mn from the +2 to +3 state and formation of the more active $Mn_3(O)$ cluster complex. In the presence of cyclohexanone (solution 3), some reduction in the intensity of $Mn_3(O)$ bands was observed (Fig. 4, curve d; dilution factor = 20), suggesting that part of $Mn_3(O)$ is reconverted to Mn(II) species in the presence of cyclohexanone. The $Mn_3(O)$ cluster and Mn(II) species are, perhaps, in a quasiequilibrium.

Solution 4, containing the mixture of $Co(OAc)_2$ and $Mn(OAc)_2$ (3 : 1 mmol), exhibited *d–d* transitions in the visible region, at 524 and 490 nm, corresponding to Co(II) acetate complexes. On heating at 363 K for 45 min and pressurizing with air (700 psig) the intensity of these bands increased (Fig. 5, curves e and f). With MEK, solution 5 (700 psig, 363 K, 45 min) showed marked changes in the position and intensity of the UV–visible bands (Fig. 5, curve g; dilution = 20). New bands appeared, around 570, 455, and 345 nm. The broad band at 570 nm is due to a Co(III) species and those at 455 and 345 nm are characteristic of μ_3-oxo-bridged Co/Mn cluster complexes ($CoMn_2(O)$) (27). In the presence of cyclohexanone (solution 6) a reduction in the intensity of these bands (Fig. 5, curve h) was observed in addition to the appearance of a weak band at 524 nm corresponding to Co(II) species. The electronic spectroscopic studies of $Mn(OAc)_2$ and a mixture of $Co(OAc)_2$ and $Mn(OAc)_2$ solutions reveal that during the oxidation reaction a small number of M(III) ions in the cluster complex are reduced to M(II) species.

EPR Spectroscopy

Solution 4, containing a mixture of $Co(OAc)_2$ and $Mn(OAc)_2$, showed a resolved sextet-line hyperfine pattern ($A_{iso} = 94.5$ G) centered at $g_{iso} = 2.0012$ due to the manganese(II) acetate complex (Fig. 6, Curve a). Although Co(II) acetate is paramagnetic ($S = 3/2$), its EPR signals cannot be detected at ambient temperatures due to the short spin lattice relaxation times. When the solution was pressurized with air (700 psig at 363 K for 45 min) the overall spectral intensity decreased (Fig. 6, curve b), the signals broadened, and the spectral width increased from 524 to 538 G. The center of the hyperfine pattern shifted from $g_{iso} = 2.012$ to 1.998. These features indicate the formation of magnetically interacting Co/Mn cluster complexes ($CoMn_2(O)$) at high pressure (700 psig) and temperatures (363 K) from individual cobalt and manganese acetate salts. This result is in agreement with the electronic spectroscopic studies, wherein these cluster complexes were observed and characterized by bands at 345 and 455 nm (Fig. 5). The formal oxidation state of Mn ions also changes from +2 to +3 on the formation of the cluster complexes. When MEK was added and the system pressurized with air (700 psig, 365 K, 45 min; solution 5) a significant decrease in EPR signal intensity was observed, indicating the formation

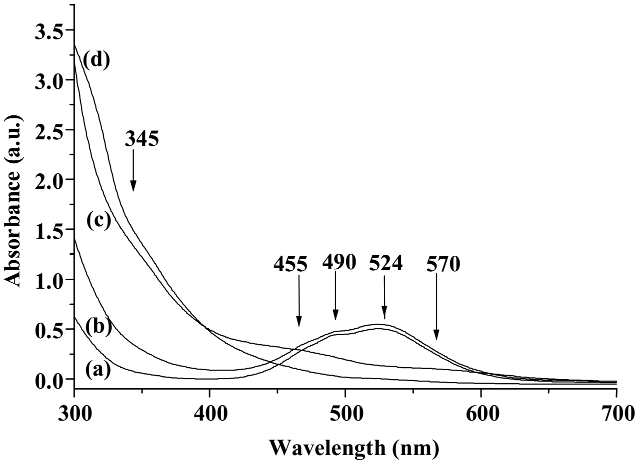

FIG. 5. Electronic spectra of cobalt and manganese complexes: (a) $Co(OAc)_2$ + $Mn(OAc)_2$ (3 : 1 mmol) in HOAc + pyridine + H_2O at 363 K, 45 min; (b) solution in (a) at 700 psig air, 363 K, 45 min; (c) $Co(OAc)_2$ + $Mn(OAc)_2$ in HOAc + pyridine + H_2O + MEK at 700 psig, 363 K, 45 min; (d) $Co(OAc)_2$ + $Mn(OAc)_2$ in HOAc + pyridine + H_2O + MEK + cyclohexanone at 700 psig, 363 K, 45 min.

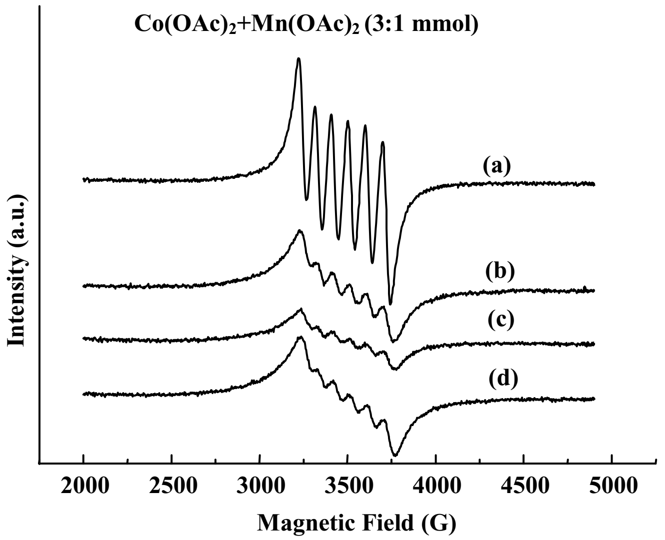

FIG. 6. EPR spectra of reaction solutions at 298 K: (a) $Co(OAc)_2 + Mn(OAc)_2$ (3 : 1 mmol) in HOAc + pyridine + H_2O at 363 K, 45 min; (b) solution in (a) at 700 psig air, 363 K, 45 min; (c) $Co(OAc)_2 + Mn(OAc)_2$ in HOAc + pyridine + H_2O + MEK at 700 psig, 363 K, 45 min; (d) $Co(OAc)_2 + Mn(OAc)_2$ in HOAc + pyridine + H_2O + MEK + cyclohexanone at 700 psig, 363 K, 45 min.

of the EPR-silent μ_3-oxo-bridged Co/Mn clusters (Fig. 6, curve c). When cyclohexanone was added (solution 6), the overall intensity increased (solution 6; Fig. 6, curve d) due to partial decomposition of the cluster complexes to monomeric Co(II) and Mn(II) species. Similar conclusions were drawn also from the electronic spectroscopic studies (see above).

Speculated Mechanism of Cyclohexanone Oxidation

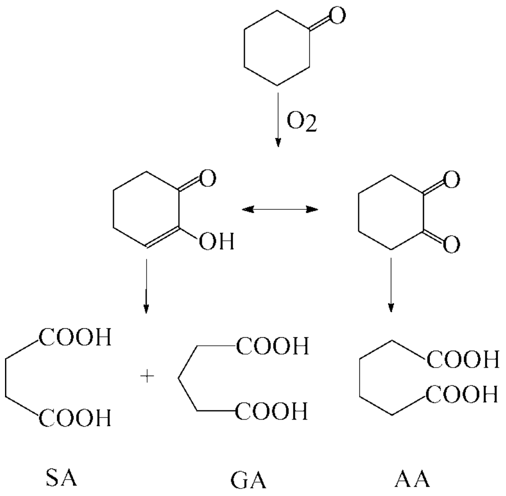

FIG. 7. Possible mechanism of cyclohexanone oxidation.

In the oxidation of cyclohexanone, 1,2-cyclohexanedione is an intermediate (Fig. 7) (1). While the keto-form yields the desired product AA, the enol-form leads to other acid impurities (1). The acid impurities (such as GA, VA, and SA) can form also by oxidative degradation of AA. A plausible mechanism for the degradation of AA is as follows (28):

$$M^{III}(OAc)_3 + HOOC(CH_2)_4COOH \leftrightarrow M^{III}(OAc)_2(OOC(CH_2)_4COOH) + HOAc, \quad [1]$$

$$M^{III}(OAc)_2(OOC(CH_2)_4COOH) \rightarrow M^{II}(OAc)_2 + CO_2 + \bullet CH_2(CH_2)_3COOH, \quad [2]$$

$$\bullet CH_2(CH_2)_3COOH + O_2 \rightarrow HOOC(CH_2)_3COOH, \quad [3]$$

$$M^{III}(OAc)_3 + HOOC(CH_2)_3COOH \leftrightarrow M^{III}(OAc)_2(OOC(CH_2)_3COOH) + HOAc, \quad [4]$$

$$M^{III}(OAc)_2(OOC(CH_2)_3COOH) \rightarrow M^{II}(OAc)_2 + CO_2 + \bullet CH_2(CH_2)_2COOH, \quad [5]$$

$$\bullet CH_2(CH_2)_2COOH + O_2 \rightarrow HOOC(CH_2)_2COOH. \quad [6]$$

Two features may be noted: (i) the decomposition of adipic to glutaric and succinic acids, and (ii) the partial reduction of the metal ions (from the tri- to the divalent state). Such a change in the oxidation state of metal ions in cyclohexanone oxidation was indeed observed by us by *in situ* electronic and EPR spectroscopic studies (*vide supra*). During the oxidation reaction, the metal ions are reoxidized by O_2.

CONCLUSIONS

A novel, non-HNO_3 route for the preparation of adipic acid by aerial oxidation of cyclohexanone or a mixture of cyclohexanone and cyclohexanol or cyclohexane using μ_3-oxo-bridged Co/Mn cluster complexes is reported. The yields of adipic acid are comparable to those in current processes.

REFERENCES

1. Davis, D. D., and Kemp, D. R., *in* "Kirk–Othmer Encyclopedia of Chemical Technology" (J. I. Kroschwitz and M. Howe-Grant, Eds.), Vol. 1, p. 466. Wiley, New York, 1991.
2. Castellan, A., Bart, J. C. J., and Cavallaro, S., *Catal. Today* **9**, 237 (1991).
3. Dumas, T., and Bulani, W., *in* "Oxidation of Petrochemicals: Chemistry and Technology." Applied Science, London, 1974.
4. Thiemens, M. H., and Trogler, W. C., *Science* **251**, 932 (1991).
5. Schuchardt, U., Cardoso, D., Sercheli, R., Pereira, R., da Cruz, R. S., Guerreiro, M. C., Mandelli, D., Spinacé, E. V., and Pires, E. L., *Appl. Catal. A* **211**, 1 (2001).
6. Scott, A., *Chem. Week.*, Feb. 18, p. 37 (1998).
7. Tanaka, K., *CHEMTECH* 555 (1974).
8. Tanaka, K., *Hydrocarbon Process.* 114 (1974).
9. Chauvel, A., Delmon, B., and Holderich, W. F., *Appl. Catal. A* **115**, 173 (1994).
10. Parton, R. F., Vankelecom, I. F. J., Casselman, M. J. A., Bezoukhanova, C. P., Uytterhoeven, J. B., and Jacobs, P. A., *Nature* **370**, 541 (1994).
11. Thisbault-Starzyk, F., Parton, R. F., and Jacobs, P. A., *Stud. Surf. Sci. Catal.* **84**, 1419 (1994).
12. Parton, R. F., Peere, G. J., Neys, P. E., Jacobs, P. A., Claessens, R., and Baron, G. V., *J. Mol. Catal. A* **113**, 445 (1996).

13. Balkus, K. J., Jr., Eissa, M., and Lavado, R., *J. Am. Chem. Soc.* **117**, 10753 (1995).
14. Balkus, K. J., Jr., Eissa, M., and Lavado, R., *Stud. Surf. Sci. Catal.* **94**, 713 (1995).
15. Herron, N., Stucky, G. D., and Tolman, C. A., *J. Chem. Soc. Chem. Commun.* 1521 (1986).
16. Raja, R., and Ratnasamy, P., *Catal. Lett.* **48**, 1 (1997).
17. Raja, R., and Ratnasamy, P., U.S. Patent 5,767,320 (1998).
18. Sato, K., Aoki, M., and Noyori, R., *Science* **281**, 1646 (1998).
19. Dugal, M., Sankar, G., Raja, R., and Thomas, J. M., *Angew. Chem. Int. Ed.* **39**, 2310 (2000).
20. Raja, R., Sankar, G., and Thomas, J. M., *Angew. Chem. Int. Ed.* **39**, 2313 (2000).
21. Thomas, J. M., Raja, R., Sankar, G., and Bell, R. G., *Nature* **398**, 227 (1999).
22. Luna, F. J., Ukawa, S. E., Wallau, M., and Schuchardt, U., *J. Mol. Catal. A* **117**, 405 (1997).
23. Chavan, S. A., Halligudi, S. B., Srinivas, D., and Ratnasamy, P., *J. Mol. Catal. A* **161**, 49 (2000).
24. Chavan, S. A., Srinivas, D., and Ratnasamy, P., *Chem. Commun.* 1124 (2001).
25. Chavan, S. A., Srinivas, D., and Ratnasamy, P., *J. Catal.* **204**, 409 (2001).
26. Partenheimer, W., *Catal. Today* **23**, 69 (1995).
27. Vincent, J. B., Chang, H.-R., Folting, K., Huffman, J. C., Christou, G., and Hendrickson, D. N., *J. Am. Chem. Soc.* **109**, 5703 (1987).
28. Schulz, J. G. D., and Onopchenko, A., *J. Org. Chem.* **45**, 3716 (1980).